

Flow topology around a 6-row vertical agrivoltaic power plant

Darteville J.¹, Bruhwyl R.¹, Lebeau F.¹¹ DEAL, BioDynE, Gembloux Agro-Bio Tech, Université de Liège

Agri-PV and microclimate

Agrivoltaics, the combination of agricultural production and photovoltaic energy generation on the same land, is emerging as a promising strategy to address both climate change mitigation and sustainable land use [1,2]. Among its various configurations, vertical inter-row agrivoltaic systems are gaining popularity for their capacity to preserve productive farmland while supporting energy goals [3]. These systems consist of alternating rows of crops and vertically mounted PV panels, often spaced by several meters adequate light penetration and access for machinery.

Understanding the flow

- Air movement strongly influences **microclimatic variables** and **turbulence transport** of specific and latent heat [4,5].
- Moreover, the flow topology determines aerodynamic forces acting on the panels, which directly impact structural design.
- The **windbreak effect** created by vertical PV rows can also reduce wind stress on crops and protect them from mechanical damage [1].

This study focuses on the airflow patterns around a 6-row vertical agrivoltaic demonstrator with a wind facing the panels, with the aim of gaining insight into the aerodynamic behavior of the system. This configuration allows us to use 2D simulations. The ultimate goal is to better understand how such infrastructure interacts with its environment, particularly the crop layer, and to contribute to the design of more efficient, resilient, and sustainable agrivoltaic systems.

Materials and Methods

This study is based on 2D numerical simulations based on Computational Fluid Dynamics (CFD) that represent a 6-rows vertical agrivoltaics power plant (see Figure 1) when the panels face the flow. The system features vertical bifacial panels spaced 10 meters apart, with a clearance height of approximately 0.8 meters and a total panel height of just over 2 meters. The study was conduct using the open-source software OpenFoam to simulate the wind with a (Reynolds Averaged Navier-Stokes) RANS model completed by source and sink terms to represent the plant canopy. The turbulence was modelled by the $k - \omega$ SST model for its capacity to well represent turbulence in case of flow separation and adverse pressure (Menter & Esch, 2001).

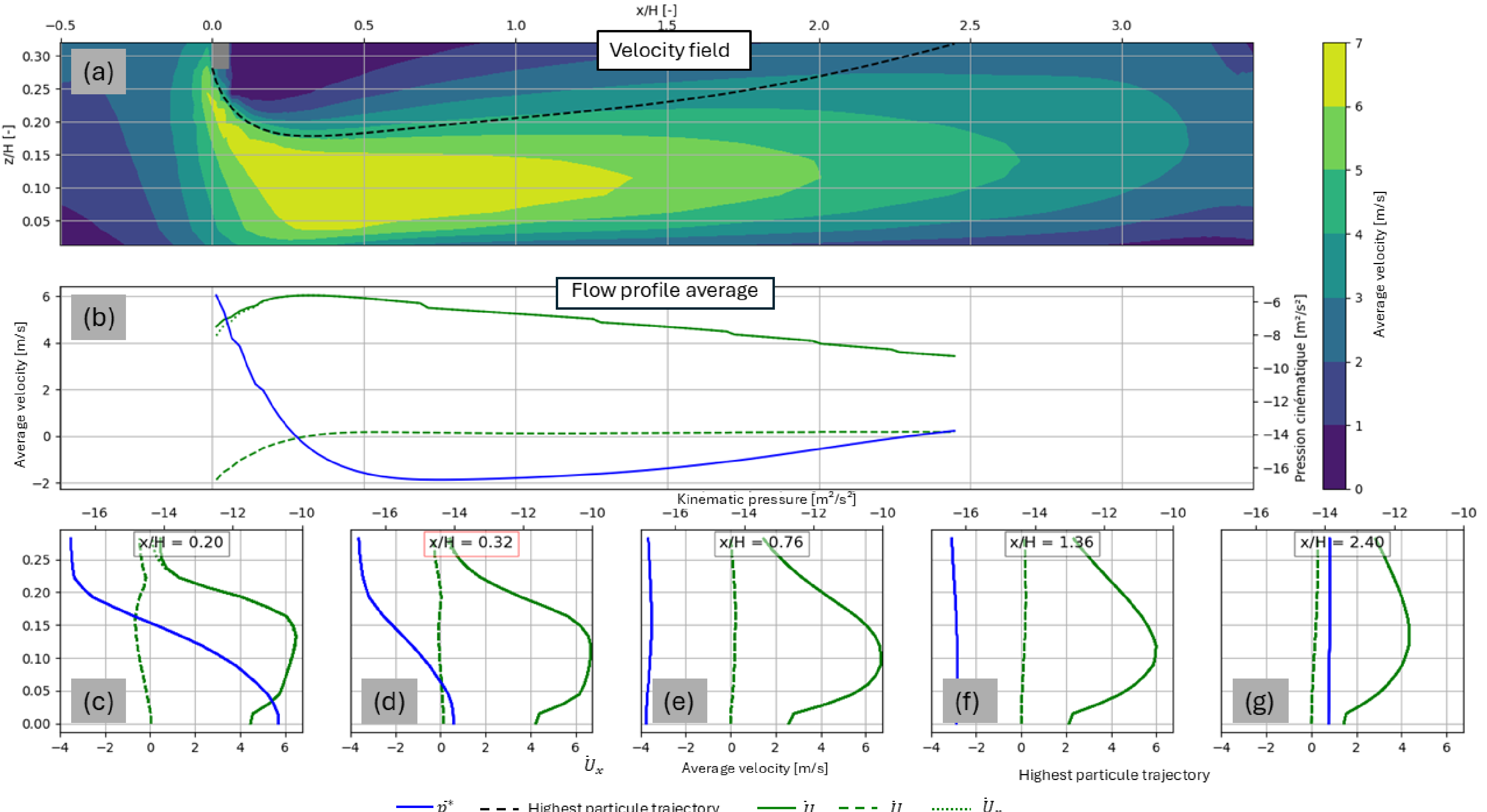


Figure 3: Caractérisation of the Venturi effect under the first panel. (a) Field of the velocity magnitude in the normalized coordinates ; Grey rectangle: bottom of the first panels; Black dashed line: Highest particule trajectory that passed below the panel (channeling between this line and the ground); (b) Profile average under the black dashed line in the subfigure a. Blue line: kinematic pressure in m^2/s^2 ; Solid green line: velocity magnitude in m/s , Dashed green line: vertical velocity component in m/s ; Dotted green line: horizontal velocity component m/s ; (c) – (g) velocity and pressure profiles at different x location. The title indicates the location; Red rectangle: maximum velocity location.

Take home message

- CFD analysis of the flow field in a growing crop conditions in an 6 rows Agri-PV power plant.
- Important flux separation caused by the panels: use of an appropriate turbulence closure model $k - \omega$ SST
- A pronounced Venturi-type contraction develops under the first PV row; its magnitude controls near-ground wind speed, pressure and turbulence and can affect the growing of the crops.
- Future work: 3D implementation, use of Large Eddy Simulation to resolve the turbulence, validation.

Results

The simulations reveal a pronounced inertial contraction under the first panel row, forming a “Venturi effect” that channels airflow and increases velocity near the ground (Figure 3-5). Bare soil conditions exhibit the strongest contraction, with high horizontal wind speeds near the surface. As vegetation develops, the aerodynamic resistance increases, reducing the wind speed and shifting the location of maximum contraction upstream. The flowering and ripening stages show the greatest dampening effect due to their higher canopy density. Across all configurations, the contraction depend mainly on crop stage. These results highlight the importance of accounting for vegetation in the design and optimization of agrivoltaic layouts.

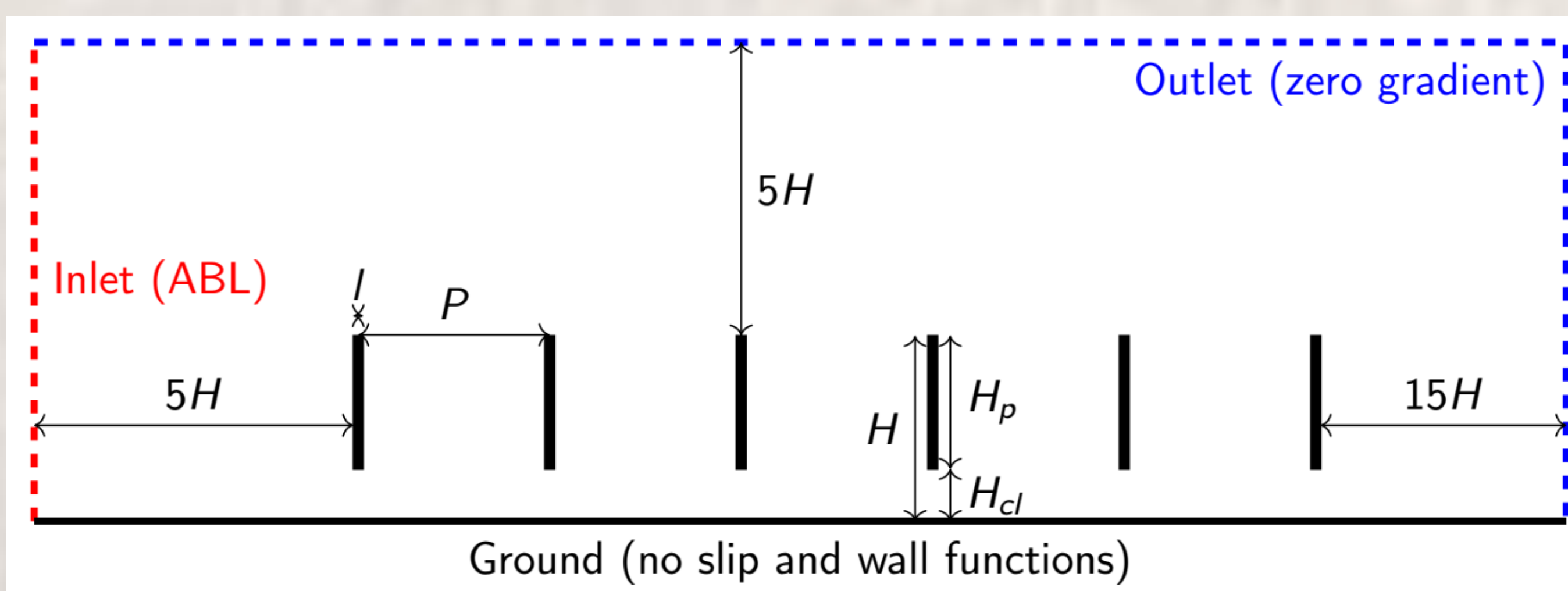
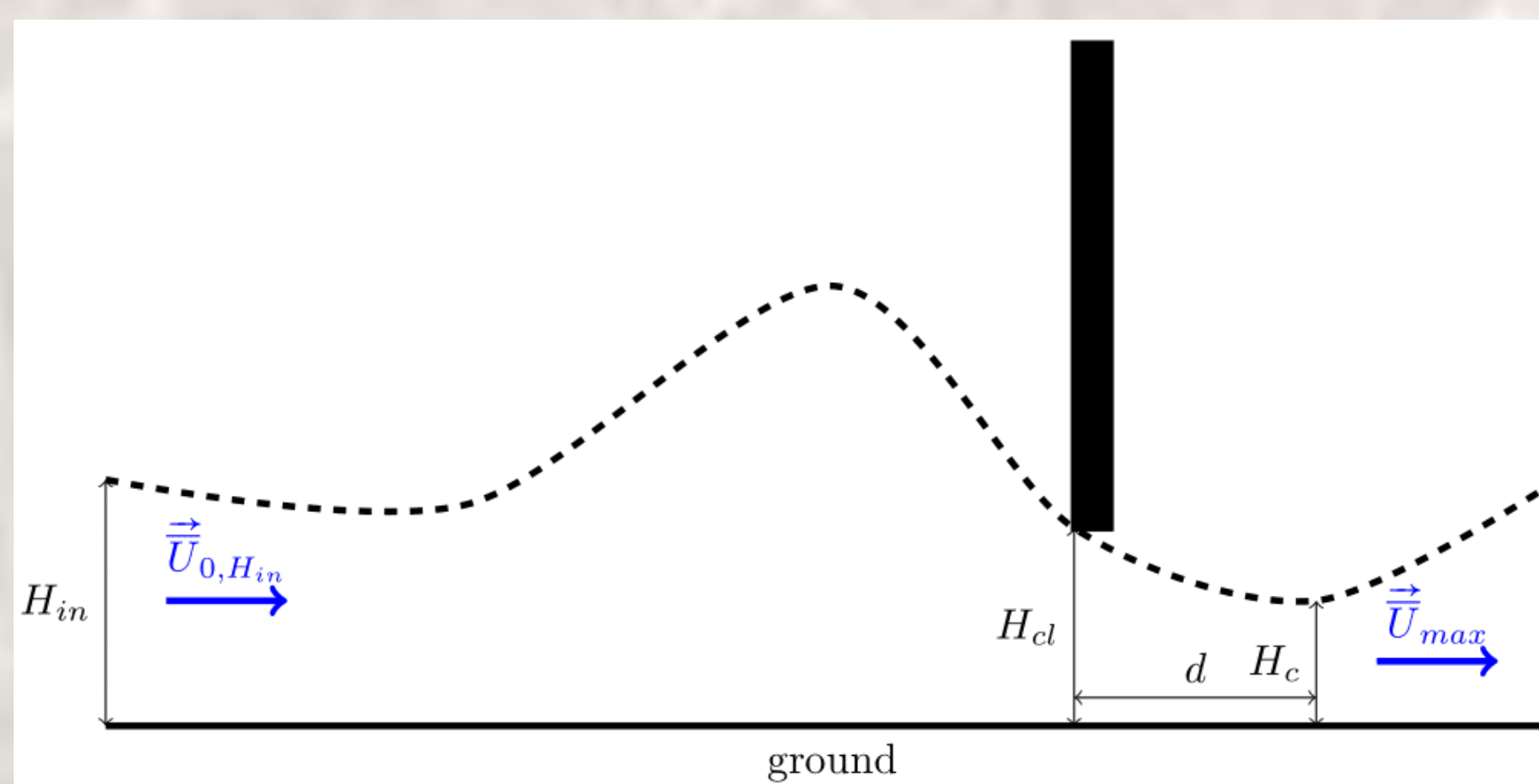


Figure 1 : Schematic diagram of the simulation domain and position of the solar panels. The red line indicates the position of the inlet. The blue lines indicate the outlet. P is the pitch distance (10 m). H_p is the panel height (2.087 m). H_{cl} is the clearance height (0.817 m). l is the row width (15cm).

A non-cartesian structured grid was generated using the blockMesh utility in OpenFOAM. The number of cells (80 000) was chosen after a grid convergence study.



For the figure 2 we can define the following equations:
Trajectory: $\frac{dx}{u_x} = \frac{dy}{u_y}$
Contraction ratio: $C_r = \frac{H_{cl}}{H_{in}}$
Max vel.: $\bar{U}_{max,x} = \frac{\int_0^{H_{in}} U_{in} dz}{H_c}$
By ‘leasing’ a particule forward and backward from the lower left corner of the panel, the trajectory (that is that coincides with the streamline in case of RANS model) can be computed by integrating the trajectory equation.

Figure 2 : Schematic diagram of venturi effect under the first panel and its relation with the inlet profile. Black rectangle: first panel; Black dashed line: Highest particule trajectory passing under this first panel. d: Distance of the vena contracta with the first panel; H_c : contraction height; H_{in} : inlet height participating to the venturi flow.

Five different crop canopy stages were tested: bare soil, tillering stage, elongation stage, flowering stage and ripening stage. Plant parameters were based on data from [7, 8] and the canopy methodology of [9] with 20 different inlet wind velocity (ranging from 1 to 20 m/s measured at 2 meters height).

References

- [1] ADEME, I Care & Consult, Ceresco, and Cétiac, *Caractériser les projets photovoltaïques sur terrains agricoles et l'agrivoltaïsme – Guide de classification des projets et définition de l'agrivoltaïsme*, Technical Report, 2021.
- [2] S. Gorjian, E. Bousi, Ö. E. Özdemir, M. Trommsdorff, N. M. Kumar, A. Anand, K. Kant, and S. S. Chopra, “Progress and challenges of crop production and electricity generation in agrivoltaic systems using semi-transparent photovoltaic technology,” *Renewable and Sustainable Energy Reviews*, vol. 158, p. 112126, Apr. 2022, doi: 10.1016/j.rser.2022.112126.
- [3] A. Chatzipanagiotis, N. Taylor, and A. Jaeger-Waldau, “Overview of the potential and challenges for Agri-Photovoltaics in the European Union,” *European Commission JRC*, Apr. 2023, [Online]. Available: <https://publications.jrc.ec.europa.eu/repository/handle/JRC132879>
- [4] J. Coombs, D. O. Hall, S. P. Long, and J. M. O. Scurlock, *Techniques in Bioproduction and Photosynthesis*, 2nd ed. Oxford: Pergamon Press, 1985.
- [5] J. C. Kaimal and J. J. Finnigan, *Atmospheric Boundary Layer Flows: Their Structure and Measurement*. Oxford University Press, 1994.
- [6] F. Menter and T. Esch, “Elements of industrial heat transfer predictions,” in *Proc. 16th Brazilian Congress of Mechanical Engineering*, vol. 20, p. 11, Uberlândia, 2001.
- [7] F. Hosoi and K. Omata, “Estimating vertical plant area density profile and growth parameters of a wheat canopy at different growth stages using three-dimensional portable LiDAR imaging,” *ISPRS J. Photogramm. Remote Sens.*, vol. 64, no. 2, pp. 151–158, Mar. 2009, doi: 10.1016/j.isprsjprs.2008.09.003.
- [8] G. Wohlfahrt, S. Sapinsky, U. Tappeiner, and A. Cernusca, “Estimation of plant area index of grasslands from measurements of canopy radiation profiles,” *Agric. For. Meteorol.*, vol. 109, no. 1, pp. 1–12, Aug. 2001, doi: 10.1016/S0168-1923(01)00259-3.
- [9] A. Sogachev and O. Panferov, “Modification of two-equation models to account for plant drag,” *Boundary-Layer Meteorol.*, vol. 121, no. 2, pp. 229–266, Nov. 2006, doi: 10.1007/s10546-006-9073-5.

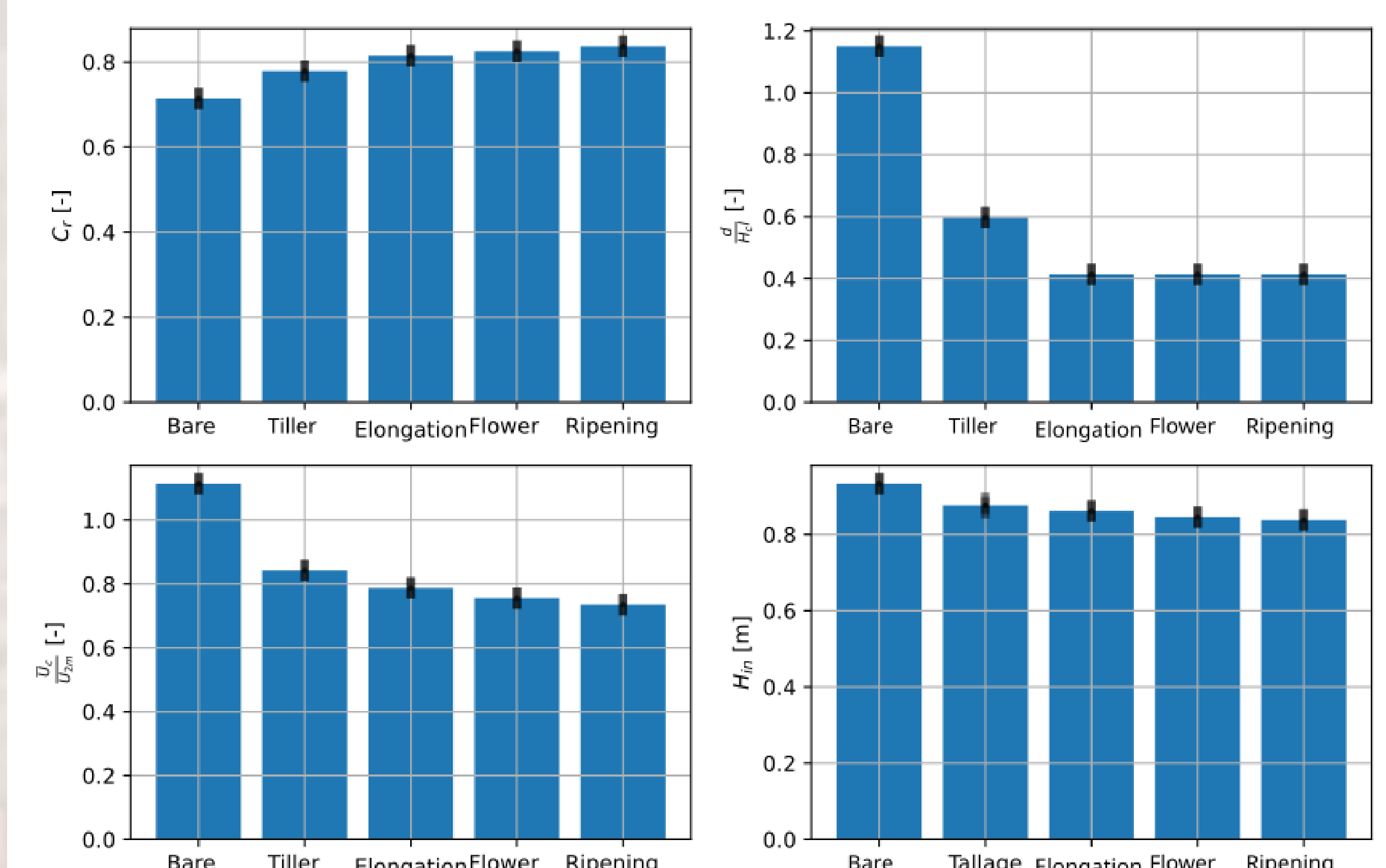


Figure 4: Influence of the crop stage on the contraction downstream the first panel. The results are averaged for 10 different inlet velocity (1 to 20 m/s). Top left: contraction ratio; Top right: normalised distance between the first panel and the maximum contraction profile; Bottom left: Ratio between the mean velocity at the maximum contraction and the inlet velocity at 2m; Bottom right: Inlet height

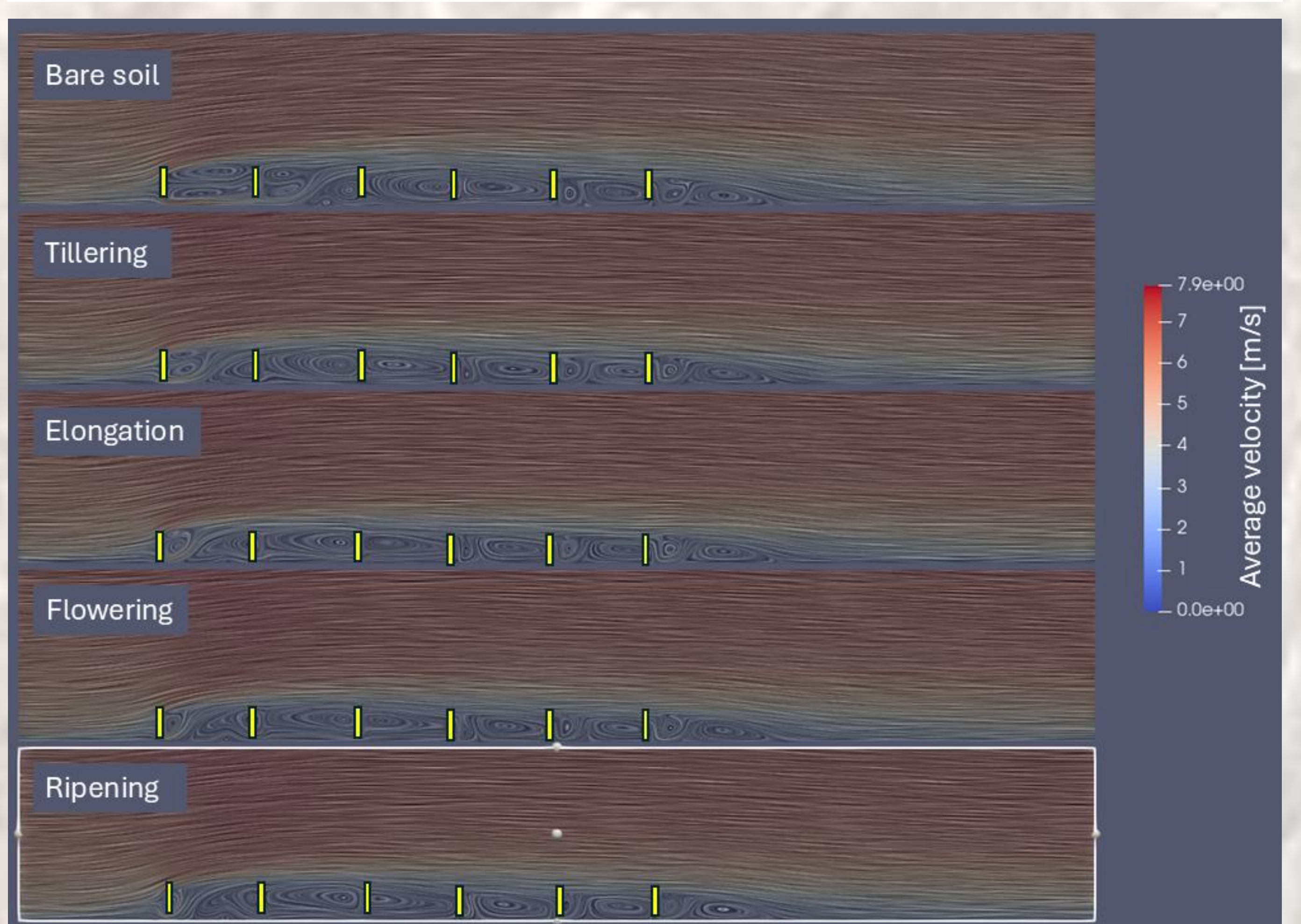


Figure 5: Velocity field with an inlet of 5 m/s at 2m for the 5 crop stage: Bare soil, Tillering, Elongation, Flowering and Ripening.